Transition from metastability to instability in the dynamics of phase separation

Amitabha Chakrabarti
Department of Physics, Kansas State University, Manhattan, Kansas 66506
(Received 30 October 1991)

We present results from a numerical study of the Cahn-Hilliard-Cook model in two dimensions. We study the transition from metastability to instability in this model by systematically changing the quench depth for an off-critical quench condition. We use different kinetic probes in the simulation to distinguish between two types of growth mechanisms: nucleation and spinodal decomposition. Although we can distinguish between nucleation and spinodal decomposition in some cases, the transition between these two growth processes is gradual. We do not see any evidence of a sharp transition from one to the other at the mean field spinodal line. Actually, the center of the diffuse transition zone that we find in the simulation is located above the mean-field spinodal line. These features of the transition zone agree extremely well with analytical theories and with recent experiments.

I. INTRODUCTION

The dynamics of phase separation in systems like metal alloys, fluid mixtures, and polymer blends is of great theoretical and practical interest.[1,2] One usually makes a distinction between two very different mechanisms of evolution during such a phase-separation process. If the system is quenched from a high-temperature single-phase region to a point inside the metastable part of the phase diagram, i.e., between the coexistence curve and the so-called spinodal line, it evolves by nucleation of the minority phase and subsequent growth of the nuclei formed. On the other hand, if the system is quenched to a point between the spinodal curve and the center of the phase diagram, it becomes unstable against long-wavelength instabilities and evolves by spinodal decomposition.

In the mean-field-type theory,[1,2] the transition between nucleation-growth (NG) and spinodal decomposition (SD) is sharp and separated by the (mean-field) spinodal line. However, when statistical fluctuations are taken into account, theoretical calculations[2-4] show that the spinodal line gets smeared out and the transition from nucleation and growth to spinodal decomposition becomes diffuse in models with short-range interactions. The general picture of a diffuse spinodal line predicted in the theory is supported by numerical simulation of Ising models.[5] However, no systematic calculation is available to predict how the kinetics of the phase-separation process should change as a function of quench depth, as one quenches the system at different points on each side of the mean-field spinodal line.

In this paper, we carry out a numerical simulation of the Cahn-Hilliard-Cook (CHC) model[1] in two dimensions to study the transition in the dynamics of the phase-separation process as the system is quenched at different locations across the mean-field spinodal curve. The motivation of this calculation comes from a recent experimental study[6] of phase separation in a viscous liquid mixture, where a diffuse metastable to unstable crossover phenomenon has been observed in the early to intermediate time regime. Since the CHC model is used in the literature as a prototype model for theoretical study of phase separation,[1,7-9] it is interesting to study the nature of such a transition in this model for intermediate time regimes, where the linear theory of phase separation breaks down and nonlinear effects become important.

In the numerical simulation reported here, we systematically change the quench depth under an off-critical quench condition. We study the dynamical evolution of the system in the early to intermediate time regime at each quench location and try to determine whether the phase-separation process is controlled by a NG-type mechanism or by a SD-type mechanism. Since the numerical simulation is carried out in two dimensions, the minority phase is below the percolation threshold for any off-critical quench. In the intermediate time, then, we find that even if the system is clearly inside the unstable region, the interconnected structure usually associated with spinodal decomposition is absent in the simulation. As a result, the morphology of the phase-separated domains is always of droplet type and it is difficult to distinguish between NG and SD just from morphological evidence. Using different kinetic probes in the simulation, we find that for the off-critical quenches considered here, there is clear evidence that the phase separation is governed by a NG mechanism at some part of the phase diagram and by spinodal decomposition at some other part. We can draw such conclusions from data taken in the intermediate time regimes. Analysis of the data taken in the intermediate time regime also suggests that the transition region between the two growth mechanisms is diffuse as suggested in previous theoretical work.[2-4]

II. MODEL AND NUMERICAL PROCEDURE

In the CHC model of phase separation, one writes the time (τ) variation of the concentration field $\Psi(\mathbf{r},\tau)$ in terms of the functional derivative of a coarse-grained free-energy functional $F[\Psi]$ and a thermal noise term. Since the order parameter is conserved, one finds

$$\frac{\partial\Psi(\mathbf{r},\tau)}{\partial\tau}=M\nabla^2\frac{\delta F}{\delta\Psi}+\eta(\mathbf{r},\tau)\ , \tag{1}$$

where M is the mobility and $\eta(\mathbf{r},\tau)$ is the Gaussian noise term obeying the fluctuation dissipation relation

$$\langle \eta(\mathbf{r},\tau)\eta(\mathbf{r}',\tau')\rangle = -2Mk_BT\nabla^2\delta(\mathbf{r}-\mathbf{r}')\delta(\tau-\tau') . \quad (2)$$

The free energy $F[\Psi]$ in this model is taken to be the Ginzburg-Landau free-energy

$$\frac{F_{GL}[\Psi]}{k_BT} = \int d\mathbf{r}\left[-\frac{b}{2}\Psi^2+\frac{u}{4}\Psi^4+\frac{K}{2}|\nabla\Psi|^2\right] , \quad (3)$$

where b, u, and K are phenomenological parameters of the model. The resulting equation of motion after performing the functional derivative is

$$\frac{\partial\Psi(\mathbf{r},\tau)}{\partial\tau} = Mk_BT\nabla^2(-b\Psi+u\Psi^3-K\nabla^2\Psi)+\eta . \quad (4)$$

The above equation can be written in a simpler form by suitable rescaling. We introduce a time variable $t=\tau/(Mk_BTK)$, a field $\phi=K^{1/2}\Psi$, and parameters $\theta=b/K$ and $\chi=u/K^2$. In terms of these variables, Eq. (4) becomes

$$\frac{\partial\phi(\mathbf{r},t)}{\partial t} = \nabla^2(-\theta\phi+\chi\phi^3-\nabla^2\phi)+\xi , \quad (5)$$

where the new noise term ξ satisfies the fluctuation-dissipation relation

$$\langle \xi(\mathbf{r},t)\xi(\mathbf{r}',t')\rangle = -2\nabla^2\delta(\mathbf{r}-\mathbf{r}')\delta(t-t') . \quad (6)$$

Our simulation has focused on two-dimensional systems. In a previous study[10] we have carried out a calculation of the phase diagram of the model in two dimensions by using a heat-bath Monte Carlo method combined with extrapolation techniques.[11] We show the phase diagram in Fig. 1 by plotting θ versus the average order parameter $\langle\phi\rangle$ for $\chi=1$. In the above figure we also show the corresponding mean-field spinodal line given by

$$\theta = 3\langle\phi\rangle^2 . \quad (7)$$

We have considered both critical and off-critical quenches in our simulation. Since the phase-separation process is always controlled by spinodal decomposition for a critical quench, results for the critical quenches are very useful for comparison with those for the off-critical quenches where the phase-separation process might be the nucleation-growth type or the spinodal decomposition type, depending on the quench location. We always start from a random initial configuration of the system and do an instantaneous quench at a point inside the phase diagram given by different θ values. The critical value[10] of θ is ≈ 1.265 for $\chi=1$. For critical quenches ($\langle\phi\rangle=0$) we have chosen $\theta=1.5$, 1.7, 1.9, 2.1, and 2.3 as the final quench locations. For off-critical quenches we have fixed $\langle\phi\rangle=(\frac{2}{3})^{1/2}$ and considered different final quench locations by varying θ from 1.4 to 2.3 at an interval of 0.1 (see Fig. 1). For this choice of $\langle\phi\rangle$, the coexistence curve is located at $\theta\approx 1.45$ and the mean-field spinodal line is located at $\theta=2$.

We have carried out the numerical integration of Eq. (5) (with $\chi=1$) for a lattice of size 240^2 up to a rescaled time of $t=1000$. We have used a simple Euler scheme[12]

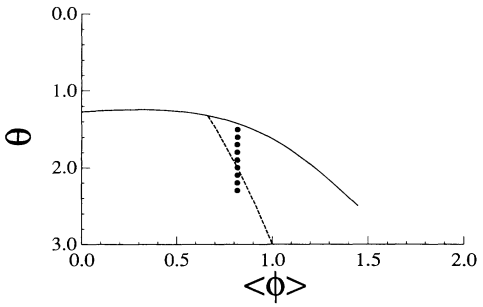

FIG. 1. The phase diagram of the two-dimensional model studied here (see text) for $\chi=1$. This phase diagram is obtained in Ref. 10. The dotted line is the mean-field spinodal curve. The solid circles denote the off-critical quench locations studied in this work.

for the numerical integration and used a time step of $\Delta t=0.025$ and a mesh size equal to unity which would correspond to a model with short-range interaction.[13] We have chosen the initial configuration of $\phi(\mathbf{r},t)$ to be Gaussian distributed with the center at $\langle\phi\rangle$ and with a variance 0.1. In order to average over the initial random configurations and the thermal noise, we have performed 20 runs at each quench location.

III. RESULTS

In Figs. 2(a)–2(c) we show the characteristic morphology of the phase-separated domains for off-critical quenches at $t=1000$ for $\theta=1.6$, 1.9, and 2.3. In these pictures the minority phase is denoted dark, i.e., wherever $\phi(\mathbf{r}, t=1000)$ took a value less than zero we put a dark dot at that $\mathbf{r}$. Since the system is still in the relatively early stage of evolution, the domains are separated by diffuse interfaces. The structure of the interface is somewhat lost in the above figures though, due to the sharp cutoff used between the black and white in the drawing. However, one can still make a few general observations from the above pictures. For $\theta=1.6$, one finds many single-particle nuclei of the minority phase due to large thermal fluctuations. As θ increases, more well-developed droplets appear at the same time t, although there are still quite a few single-particle clusters for $\theta=2.3$. Also, the formed droplets are not circular, either.[14] These features of the domains are expected since the system is yet to enter the late time-scaling regime. As mentioned earlier, the domain morphology in the off-critical quenches considered in the simulation is always the droplet type. Thus it is difficult to distinguish between the growth mechanisms just by looking at the morphology of the phase-separating domains.

We compute the probability distribution function $P(\phi)$ at a particular time t for both off-critical and critical quenches. In Fig. 3(a) we show the results for off-critical quenches and in Fig. 3(b) we show the corresponding results for critical quenches for the same θ values. The time at which these computations are carried out is given by $t=1000$. For the off-critical quenches, we find that the peak of $P(\phi)$ at negative values ϕ (which we will call the second peak) grows gradually as θ increases. For

$\theta=1.5$ the second peak is invisible in this figure, since the volume fraction of the minority phase is quite small. This behavior is expected for nucleation at earlier times. On the other hand, for $\theta=2.3$, the bimodal nature of the distribution is clear. If we compare this figure with the corresponding Fig. 3(b), we find that the distribution in 3(b) is clearly bimodal for all quenches (which are governed by spinodal decomposition for all θ above the critical value). For the off-critical quenches then, as θ is increased, there seems to be a transition from nucleation [with a barely visible second peak of $P(\phi)$ at intermediate times] to spinodal decomposition [with a well-developed bimodal distribution of $P(\phi)$]. However, the transition is gradual and nothing spectacular happens at the mean-field spinodal ($\theta=2$). One can qualitatively estimate that the diffuse transition region is in between $\theta=1.7$ and 1.9.

We draw a similar conclusion when we analyze the data for the nonequilibrium structure factor. The structure factor is defined as

$$S(\mathbf{k},t)=\left\langle \frac{1}{N}\sum_{\mathbf{r}}\sum_{\mathbf{r}'} e^{i\mathbf{k}\cdot\mathbf{r}}[\phi(\mathbf{r}+\mathbf{r}',t)\phi(\mathbf{r}',t)-\langle\phi\rangle^2]\right\rangle , \quad (8)$$

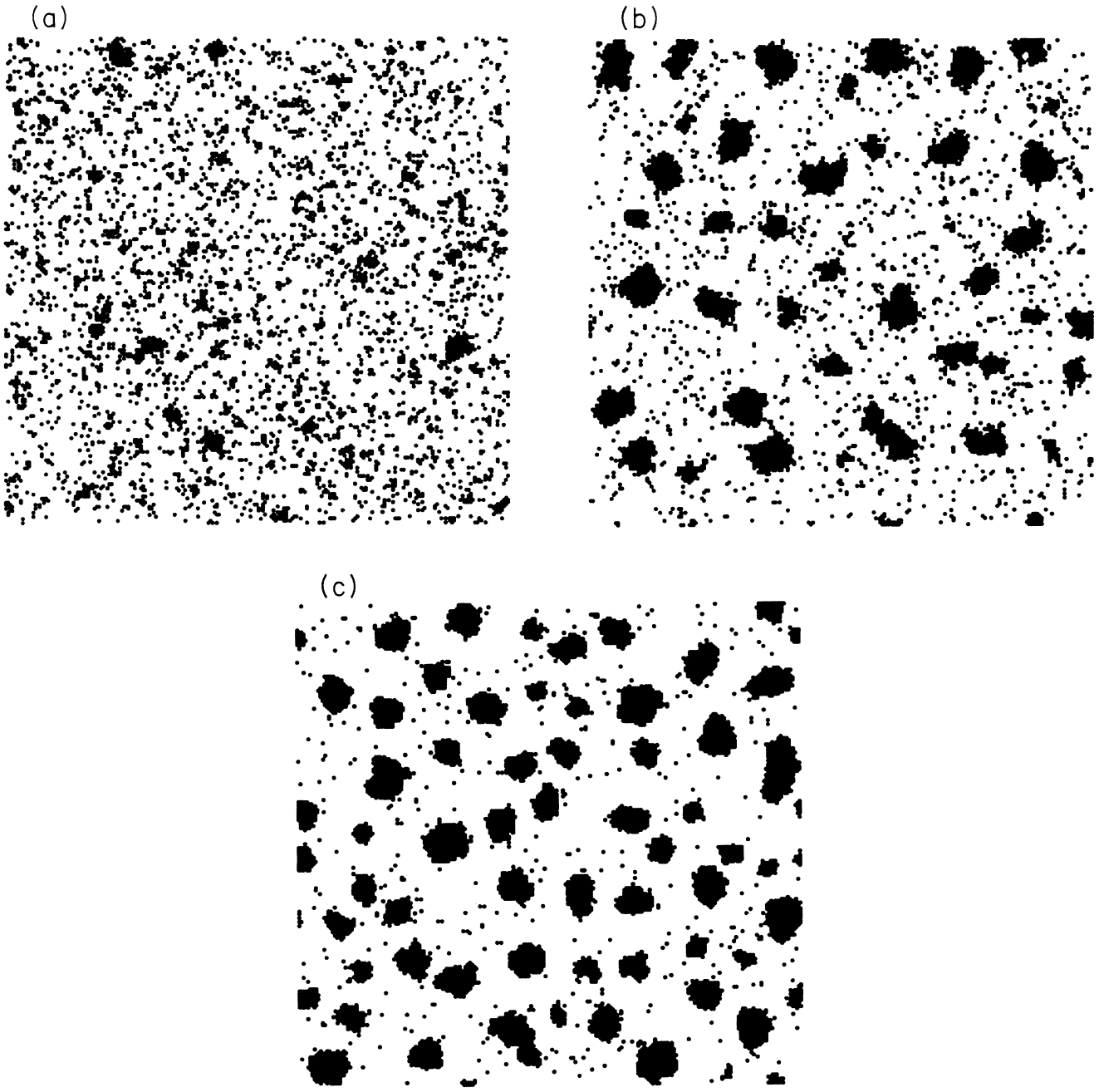

FIG. 2. (a) A typical configuration of the phase-separated domains at $t=1000$ for an off-critical quench with $\langle\phi\rangle=(\frac{2}{3})^{1/2}$ and $\theta=1.6$. (b) Same as in (a) except that $\theta=1.9$ here. (c) Same as in (a) except that $\theta=2.3$ here.

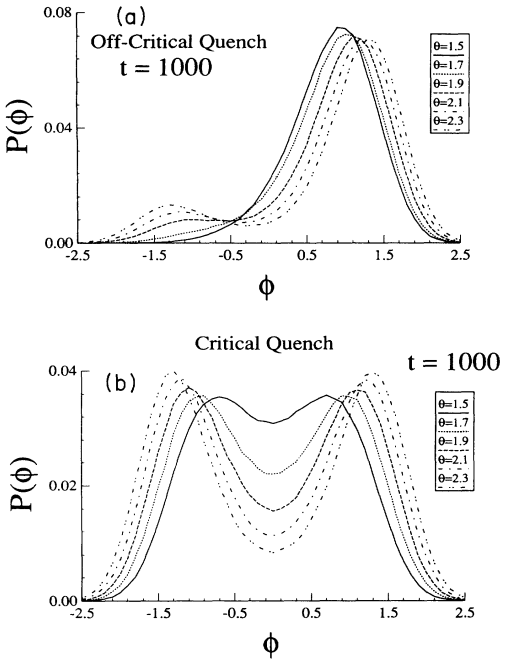

FIG. 3. (a) Probability distribution function $P(\phi)$ at $t=1000$ for off-critical quenches for different θ values. (b) Same as in (a) except for critical quenches.

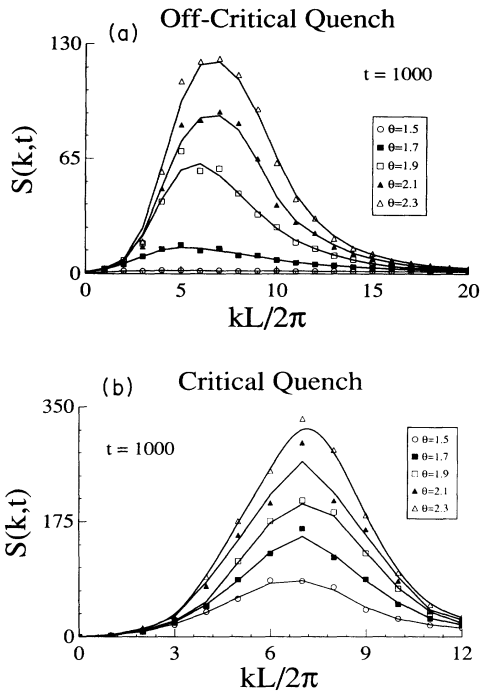

FIG. 4. (a) Circularly averaged structure factor $S(k,t)$ at $t=1000$ for off-critical quenches for different θ values. The solid lines in this and other figures are guides to the eye. (b) Same as in (a) except for critical quenches.

where the sum is over the lattice and N is the total number of lattice points. In the simulation we consider the circularly averaged structure factor $S(k,t)$. In Figs. 4(a) and 4(b) we plot $S(k,\ t=1000)$ for different θ for off-critical and critical quenches, respectively. For off-critical quenches, the peak of the structure is barely visible for $\theta=1.5$. The peak, however, increases gradually as θ is increased. On the other hand, for critical quenches, the peak is already well developed for $\theta=1.5$. In this respect, the situation is quite similar to the case of the probability distribution function $P(\phi)$ discussed before. Thus, again we find evidence of a gradual transition from nucleation to spinodal decomposition as θ is increased in the off-critical quenches.

The peak and different moments of the structure factor are accessible in experiments. As we present shortly, these quantities also carry the signature of a diffuse transition. We define a moment k_a of the structure factor as

$$k_a=\frac{\sum_k kS(k,t)}{\sum_k S(k,t)}\ , \tag{9}$$

and in Fig. 5 we plot k_a vs θ for off-critical quenches and for $t=250$ and $t=1000$. The corresponding graphs for the peak of the structure factor $S_{\max}$ vs θ are shown in Fig. 6. As θ increases $S_{\max}$ (or k_a) shows little change initially ($\theta\leq 1.7$). Subsequently, it passes through what looks like an inflection point around $\theta\approx 1.8-1.9$ and then finally becomes flat again for even larger values of θ. This suggests a clear but diffuse transition in kinetics of domain growth from nucleation (which we estimate to occur for $\theta\leq 1.7$) to spinodal decomposition (which we estimate to occur for $\theta\geq 1.9$). We note that this behavior of $S_{\max}$ as a function of quench depth is very similar to what has been found in recent experiment by Tanaka *et al.*[6]

Next we focus our attention on the nonequilibrium pair-correlation function $g(\mathbf{r},t)$, defined as

$$g(\mathbf{r},t)=\sum_{\mathbf{k}} e^{i\mathbf{k}\cdot\mathbf{r}}S(\mathbf{k},t)\ . \tag{10}$$

In this case also we consider the circularly averaged quantity $g(r,t)$ in the simulation. In Figs. 7(a) and 7(b) we plot $g(r,\ t=1000)$ vs $\mathbf{r}$ for different θ values used in off-critical and critical quenches. For critical quenches [Fig. 7(b)], the correlation function shows an oscillatory

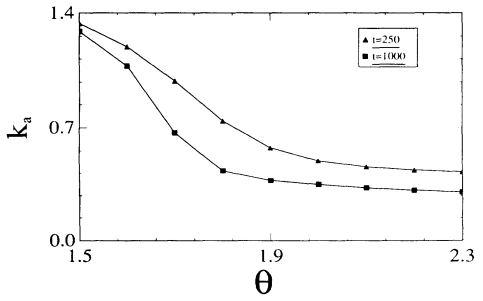

FIG. 5. Moment k_a of the circularly averaged structure factor $S(k,t)$ at $t=250$ and 1000 for off-critical quenches for different θ values.

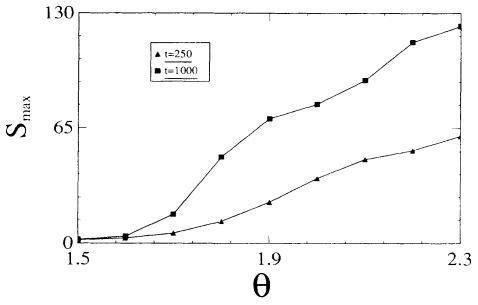

FIG. 6. Peak S_{max} of the circularly averaged structure factor $S(k,t)$ at $t=250$ and 1000 for off-critical quenches for different θ values.

behavior for all values of θ considered here. For off-critical quenches with $\theta \geq 1.9$ the correlation function shows such an oscillation. On the other hand, for $\theta \leq 1.7$ the correlation function is quite flat after its first zero. This behavior is also found in a recent simulation[15] of domain growth in the *nucleation regime*. Thus, we can conclude that the phase separation is the NG type for $\theta \leq 1.7$ and there is a gradual transition to SD if θ is further increased.

A measure of domain size used in the literature[7] is the location (R_g) of the first zero of $g(r,t)$. In Fig. 8(a) we plot R_g vs θ for off-critical quenches at two times. The transition from NG to SD is clearly visible in this figure. R_g increases with increasing θ initially, then passes through a broad peak around $\theta \approx 1.8$, and finally appears to take a constant value. We conclude that the system is undergoing nucleation and growth for those values of θ where R_g is sharply increasing (i.e., $\theta \leq 1.7$). On the other hand, the system is undergoing spinodal decomposition for those values of θ where R_g is apparently constant (i.e. $\theta \geq 2.0$). The broad peak at around $\theta \approx 1.8$ suggests a diffuse transition from NG to SD. The fact that we associate spinodal decomposition with a constant value of R_g is supported by the corresponding graph of R_g vs θ for critical quenches [Fig. 8(b)] where we find R_g to be almost independent of θ at both $t=250$ and 1000.

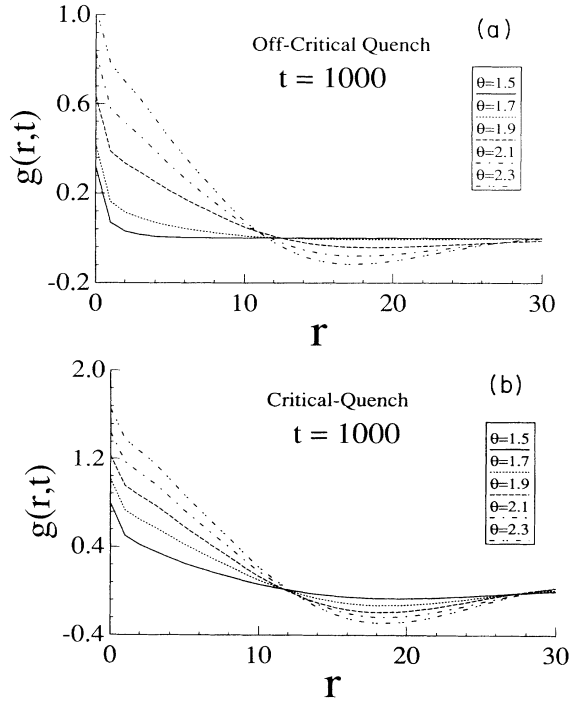

FIG. 7. (a) Circularly averaged pair-correlation function $g(\mathbf{r},t)$ at $t=1000$ for off-critical quenches for different θ values. (b) Same as in (a) except for critical quenches.

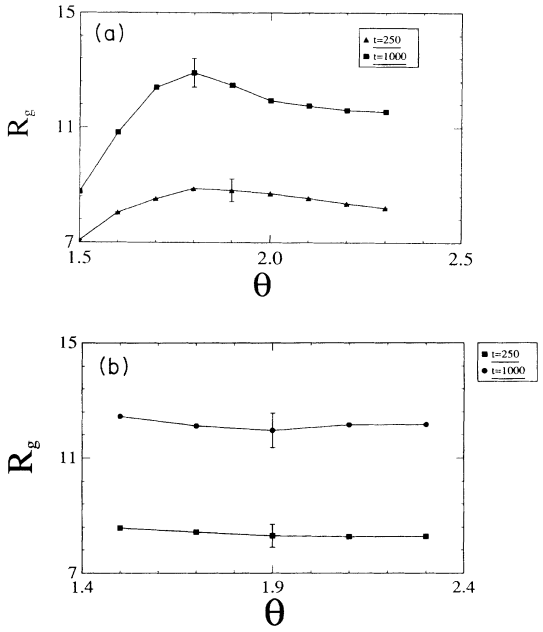

FIG. 8. (a) A measure of the average domain size R_g vs θ at $t=250$ and 1000 for off-critical quenches. Typical error bars are also shown in the figure. (b) Same as in Fig. 7(a) except for critical quenches.

We also compute the effective exponent of domain grown (n_{eff} for off-critical quenches at different θ values. One can define an effective exponent by writing the average domain size $R(t) \approx at^{n_{\text{eff}}}$. This effective exponent is computed in two different ways: (1) from values of R_g at two times $t=1000$ and 250 and (2) from values of k_a at those two times. The corresponding results are plotted in Fig. 9. Although the asymptotic growth exponent is $\frac{1}{3}$ both in the NG and SD regimes,[7-9,16,17] the effective ex-

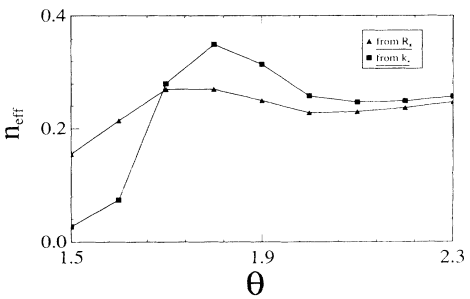

FIG. 9. The effective exponent n_{eff} calculated from R_g and k_a vs θ for off-critical quenches. The effective exponent is calculated from data at two times: $t=250$ and 1000.

ponent[18] at intermediate times could well be smaller than the above value. The effective exponent is quite small in the intermediate time regime for NG possibly due to the weak interaction among the droplets. For SD the effective exponent is smaller than the asymptotic value due to the presence of strong surface diffusion at intermediate times.[18,19] We note that the effective exponents calculated both from R_g and k_a increase with θ, go through a maximum, and then finally settle down to a lower value. A similar behavior has been seen in the R_g vs θ graph [Fig. 8(a)] but not in the k_a vs θ plot (Fig. 5). Similar to the results for R_g vs θ, here also one can draw a conclusion of gradual transition from NG to SD from the above plots, although we note that the estimated error bars to these effective exponents are quite large.

IV. SUMMARY AND CONCLUSION

In this paper we present results from a numerical study of the Cahn-Hilliard-Cook model in two dimensions, where we investigate the transition from metastability in this model. We study the dynamics of the phase-separation process by systematically changing the quench depth for an off-critical quench condition. We use different kinetic probes in the simulation to distinguish between two types of growth mechanism, namely, nucleation and growth and spinodal decomposition. We also carry out simulations for critical quenches to compare with the data for the off-critical quenches.

Although the phase-separated domains have droplet-type morphology for all the off-critical quenches considered in the simulation, analysis of our data taken in the intermediate time regime clearly shows that there are regions of the phase diagram which are metastable and the phase separation in those parts is governed by nucleation of the minority phase. On the other hand, the phase separation is controlled by spinodal decomposition at other parts of the phase diagram. It is interesting to note that this distinction is possible from data taken in the intermediate time regime where the nonlinear effects affect the dynamics considerably, whereas the theoretical concepts in the "classical" picture are developed from linear-type analysis.[1,2] Although we can distinguish between nucleation and spinodal decomposition for some values of the parameter θ, the transition between these two growth processes are gradual. We do not see any evidence of a sharp transition from one to the other at the mean-field spinodal line. Actually, the center of the diffuse zone that we find in the simulation seems to be located above the mean-field spinodal line. These features of the transition zone agree extremely well with analytical theories[2–4] and with recent experiments.[6]

ACKNOWLEDGMENTS

Acknowledgement is made to the Donors of the Petroleum Research Fund, administered by the American Chemical Society, for support of this work. The computations are made possible by a grant of computer time in the Cray-YMP computer at the NCSA Supercomputing Center. This work is also partially supported by NSF Grant No. DMR-9100245.

[1]For a review, see J. D. Gunton, M. San Miguel, and P. S. Sahni, in *Phase Transitions and Critical Phenomena,* edited by C. Domb and J. L. Lebowitz (Academic, London, 1983), Vol. 8.

[2]K. Binder, in *Phase Transformation in Materials,* edited by P. Haasen, Materials Science and Technology Vol. 5 (VCH, Weinheim, Germany, 1990), p. 405.

[3]K. Binder, Ann Phys. (N. Y.) **98**, 390 (1976); Phys. Rev. A **29**, 341 (1984); Physica (Amsterdam) **140A**, 35 (1986).

[4]K. Binder, in *Alloy Phase Stability,* edited by G. M. Stocks and A. Gonis (Kluwer, Academic, Dordrecht, 1989), p. 233.

[5]D. Heerman, W. Klein, and D. Stauffer, Phys. Rev. Lett. **49**, 1262 (1982).

[6]H. Tanaka *et al.,* Phys. Rev. Lett. **65**, 3136 (1990).

[7]For a review of recent numerical studies see, for example, J. D. Gunton, R. Toral, and A. Chakrabarti, Phys. Scr. T **33**, 12 (1990).

[8]T. M. Rogers, K. R. Elder, and R. C. Desai, Phys. Rev. B **37**, 9638 (1988); E. T. Gawlinski, J. D. Gunton, and J. Viñals, *ibid.* **39**, 7266 (1989).

[9]A. Chakrabarti, R. Toral, and J. D. Gunton, Phys. Rev. B **39**, 4386 (1989); R. Toral, A. Chakrabarti, and J. D. Gunton, Phys. Rev. Lett. **60**, 2311 (1988); Phys. Rev. B **39**, 901 (1989).

[10]R. Toral and A. Chakrabarti, Phys. Rev. B **42**, 2445 (1990).

[11]A. Ferrenberg and R. Swendsen, Phys. Rev. Lett. **61**, 2635 (1988); Phys. Rev. Lett. **63**, 1195 (1989).

[12]See, for example, T. C. Gard, *Introduction to Stochastic Differential Equations* (Dekker, New York, 1988).

[13]The effect of changing mesh size on the parameters of this model has been discussed in Ref. 10.

[14]D. Heerman and W. Klein, Phys. Rev. Lett. **50**, 1062 (1983).

[15]A. Chakrabarti, R. Toral, and J. D. Gunton, Phys. Rev. B **44**, 12 133 (1991).

[16]A. J. Bray, Phys. Rev. Lett. **62**, 2841 (1989).

[17]G. F. Mazenko, Phys. Rev. Lett. **63**, 1605 (1989).

[18]D. A. Huse, Phys. Rev. B **34**, 7845 (1986).

[19]H. Furukawa, Adv. Phys. **34**, 703 (1985).